observed, and why twinning (*i.e.* with the $+b$ axes anti-parallel) does not seem to occur.

The discussion up to now has been in terms of the lattice. In an attempt to find an answer to the above questions some attention has been given to the molecular arrangement. The set of equivalent positions occupied by the molecular centres form a body-centred array, and the presumably planar molecules are tilted out of the *ac* plane by about 20°. The assumption is now made that the macrogeometric description of the relation between two portions of a composite crystal may be regarded as a basis for the description of the actual mechanism of formation—either by oriented overgrowth where the second portion grows on the existing single-crystal portion in a definite orientation, or by oriented agglutination where two single crystals stick together in a well-defined orientation relationship. The two portions are joined across a composition plane, but unlike twinning, this plane does not bear the same crystallographic relationship to the two portions. The transition from the one portion across the composition plane to the second is supposed to extend through only a few molecular planes. We have considered in some detail the following aspects: the mismatch in the repeat distance in the composition plane, the molecular arrangement in the possible composition planes and the effects of the disc-like shape of the molecule and

its tilt. (The description of the tilt has recently been revised (Strel'tsova & Struchkov, 1961)). None of these lines of attack have produced a clear indication of why the observed effects occur in preference to other possibilities. It seems likely that the reasons for this are tied up with the mechanism of growth of small crystallites and with the faults present in such a crystallite. At present not enough is known about these phenomena to attempt a complete answer.

References

BUERGER, M. J. (1945). *Amer. Min.* **30**, 469.
CAHN, R. W. (1954). *Advanc. Phys.* **3**, 363.
DRUGMAN, J. (1928). *Bull. Soc. franç. Minér.* **51**, 187.
FRIEDEL, G. (1933). *Bull. Soc. franç. Minér.* **56**, 262.
GAFNER, G. & HERBSTEIN, F. H. (1960). *Acta Cryst.* **13**, 702.
HERMION, G. F. & ANDERSON, J. C. (1944). *J. Amer. Chem. Soc.* **66**, 1801.
HERBSTEIN, F. H. (1963). *Acta Cryst.* **16**, 255.
LONSDALE, K. (1931). *Proc. Roy. Soc.* A, **133**, 536.
MARK, H. (1924). *Ber. dtsch. chem. Ges.* **57**, 1820.
NEUHAUS, A. (1951). *Fortschr. Min.* **30**, 136.
SHASKOLSKY, M. & SHUBNIKOV, N. (1933). *Z. Kristallogr.* **85**, 1.
STREL'TSOVA, I. N. & STRUCHKOV, YU. T. (1961). *J. Struct. Chem.* **2**, 296.
TULINSKY, A. & WHITE, J. G. (1958). *Acta Cryst.* **11**, 7.
WEISZ, O., COCHRAN, W. & COLE, W. F. (1948). *Acta Cryst.* **1**, 83.

Accurate Determination of Cell Dimensions from Single-Crystal X-ray Photographs

BY F. H. HERBSTEIN

National Physical Research Laboratory, Council for Scientific and Industrial Research, Pretoria, South Africa

A front-reflection Weissenberg camera can be easily converted into a back-reflection instrument by adding a simple adaptor and changing the gear ratio on the drive mechanism. Reflections can be obtained at Bragg angles up to 86°. Conventional devices for controlling crystal temperatures over a wide range have been added to the Weissenberg camera used. The errors in cell dimensions due to errors in measured reciprocal-lattice parameters, and in interatomic distances due to errors in cell dimensions, have been derived for triclinic crystals. Measurements on a number of crystals have given standard deviations for reciprocal-lattice parameters of 0·0025–0·01%.

The film mounting described by Mathieson (*Acta Cryst.* (1957), **10**, 351) has been used for normal and inclined-beam rotation photographs. The eccentricity-error extrapolation function for inclined-beam rotation photographs has been derived and tabulated. The standard deviation of identity-period measurements is about 0·1%.

These methods are illustrated by the determination of the cell dimensions of hexabromobenzene at 20 °C.

1. Introduction

Recent advances in the techniques of X-ray crystal-structure analysis make it feasible to reduce the standard deviations of measured bond lengths due to errors in measured intensities to less than 0·2% in

favourable circumstances (Cruickshank, 1960). In order that these bond lengths should be on an absolute scale, it is necessary that the errors in cell dimensions should be appreciably smaller. The importance of accurate cell dimensions has recently been demonstrated for orthorhombic sulphur (S_8): revised cell

dimensions (maximum change 0·5%) give a mean S–S distance of $2·048 \pm 0·002_4$ Å* (Caron & Donohue, 1961; Cooper, Bond & Abrahams, 1961) compared with the previous value of $2·041 \pm 0·003$ Å (Abrahams, 1961)— a change of 2·9 σ.

Single-crystal oscillation photographs (Braekken, 1929; Farquhar & Lipson, 1948) have been used for accurate cell-dimension measurements but are inconvenient to index. The front-reflection Weissenberg method (Fischmeister, 1951; Christ, 1956) does not suffer from this difficulty but has limited accuracy because reflections beyond $\theta \sim 75°$ cannot be recorded. The back-reflection Weissenberg method introduced by Buerger (1937, 1942; Buerger & Parrish, 1937) thus represents a substantial advance over other techniques. This method has not, however, found much application, presumably because it has been thought that a special camera is needed for taking the photographs. While instrumental errors are minimized if a specially constructed camera is used, it is possible to convert the ordinary commercially available front-reflection Weissenberg camera into a back-reflection instrument simply and rapidly by use of a special adaptor (Herbstein, 1957) and still obtain results of satisfactory accuracy.

The Weissenberg method does not give information about the identity period along the rotation axis of the crystal. This can be fairly accurately measured from normal and inclined-beam rotation photographs by using the film-mounting introduced by Mathieson (1957). Applications of these two techniques are described in this paper.

In the methods described above, the angular position of the reflected beam is measured. It has been emphasized recently (Löfgren, 1961) that it is better in principle to measure the angular position of the crystal. This so-called θ-method was introduced by Weisz, Cochran & Cole (1948) and has recently been applied with striking success by Bond (1960), in a measurement of the lattice parameter of Si with a reported standard deviation of a few parts per million. The θ-method has the same indexing difficulties as the ordinary oscillating-crystal method and is very tedious when photographic methods are used. Thus the methods described here have advantages when convenience and rapidity of application are more important than attainment of the very highest accuracy.

2. Back-reflection Weissenberg technique

2·1. *Conversion of front-reflection to back-reflection instrument*

The adaptor used for converting a front-reflection Weissenberg camera into a back-reflection instrument
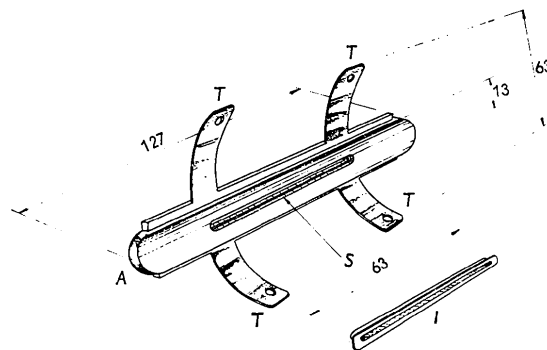
Fig. 1. Adaptor (A) for conversion of Weissenberg camera from front-reflexion to back-reflexion condition. The tabs, insert and slot mentioned in the text are denoted by T, I and S respectively. The approximate dimensions given on the figure are in millimetres.

is shown in Fig. 1.* It fits into the collimator slot of the Weissenberg film holder and is attached to the film holder by the four tabs T with the screws usually used to hold the film-retaining clips. The inner surface of the adaptor is machined to the same radius as the Weissenberg film holder and the film is held firmly against the smooth inner surface by insert I. A slit 63×3 mm is cut in $5'' \times 7''$ film with a special punch. The film is mounted in the Straumanis manner, the insert fitting into the slot S and the collimator, of 1 mm brass tubing, fitting easily through the insert.

The layer line screen is of the conventional type but is used rotated 90° away from the usual position *i.e.* with the collimator slot uppermost. Correspondingly the film is also mounted so that its free ends are at the top of the film holder. The stop for the direct beam is a slot in a brass wedge and follows Buerger's original design. The beam stop is held on an arm which is attached to the spindle-bearing of the instrument; it can be used for inclined- and normal-beam rotation photographs as well as for Weissenberg photographs. A telescope fitting on the film-holder carriage has been added to permit more accurate centring of the crystal than is possible by sighting down the collimator.

The film-holder traverse is reduced to 6 cm for a crystal oscillation of 240° by replacing the bevel gear on the driven shaft of the Weissenberg mechanism by one with half the number of teeth. Conversion of the instrument from the front-reflection to the back-reflection condition takes only a few minutes; no delicate adjustments are needed nor is the setting of the crystal in any way disturbed.

The largest values of the thermal-expansion coefficients (α) of crystals are about 2×10^{-4} (Lonsdale, 1959). As $\Delta a/a_0 = \alpha \Delta T$ a relative spacing change of 2×10^{-4} could be caused by a 1 °C. change in temper-

ature. As the standard deviations obtainable by this method are about 5×10^{-5}, it is desirable that the crystal temperature should be constant to 0·1–0·2 °C. This has been achieved, for work in the vicinity of room temperature, by blowing air that has been passed through a water-jacketed copper spiral over the crystal. For work over a wider range of temperatures, a combined heating-cooling device has been built following the design of Kreuger (1955).

2·2. *Choice of wavelength*

It is often found that central reciprocal-lattice rows do not contain enough reflections at high angles to permit the use of extrapolation techniques and general

reflections must be used. An important practical point in obtaining enough high-angle reflections is the use of X-rays of suitable wavelength: for example Fe $K\alpha$ is more useful than Cu $K\alpha$ when the temperature factor is relatively high.

2·3. *Measurement of films and derivation of* $\sin \theta$ *values*

A typical back-reflection Weissenberg photograph is shown in Fig. 2; it has a distorted scale (Buerger, 1942, p. 221–5) and central reciprocal-lattice rows make an angle of 75° 58′ with the ω-axis. The films were indexed by using a Buerger template (1942, p. 269–83) drawn to fit the present instrumental conditions (see Fig. 3).
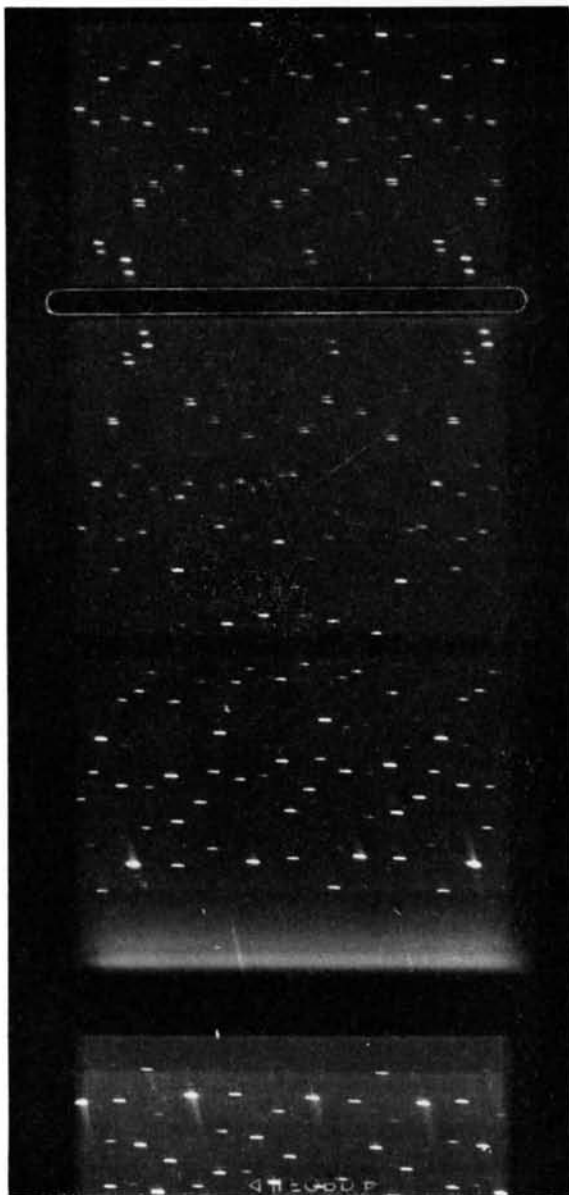
Fig. 2. Typical back-reflexion Weissenberg photograph (hexabromobenzene $h0l$ zone, Cu $K\alpha$ radiation).
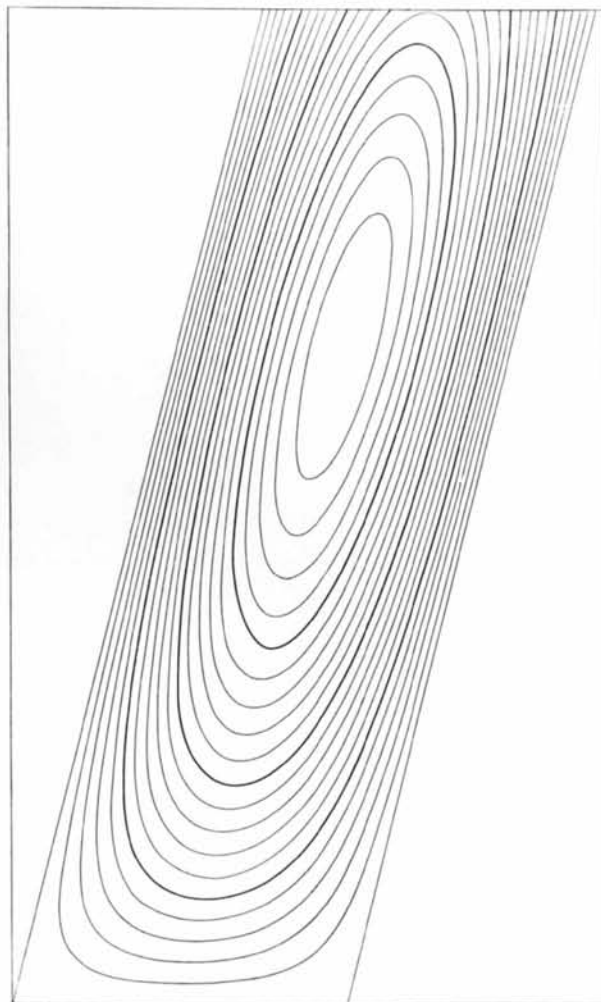
Fig. 3. Buerger template for indexing back-reflexion photographs. The camera diameter is 57·3 mm. The lines are drawn at intervals of $d^* = 0·1$, with those at 0·5, 1·0, 1·5 accentuated.

The films were measured with a Société Genèvoise d'Instruments de Physique Universal Measuring Apparatus Type MU–214 B. In this instrument the carriage holding the object to be measured can be

translated independently in two mutually perpendicular directions. This facility is needed to measure distance along the length of the film between spots situated at different points along the breadth of the film. Tests showed that the reproducibility of measuring the centre of a reflection from a needle-shaped crystal (the most favourable shape) was 0·02 mm, corresponding to an angular error of 0·02° in θ. This does not allow distinctions to be made between peak and centre-of-gravity of a reflection.

The positions corresponding to $\theta = 0°$ and 90° were found from symmetrically placed reflections in the front- and back-reflection regions and used to apply a shrinkage correction. Values of $(90 - \theta)$ were then computed for each reflection as the use of this quantity rather than θ makes any residual shrinkage correction a linear function of $\cos^2 \theta$ (Buerger, 1942, p. 419–26).

Table 1. *Wavelengths used in computations*

These wavelengths were obtained by multiplying the values given by Lonsdale (1950) by 1·000017. This factor was suggested by Parrish (1960) to take into account the latest available determinations of Avogadro's number

	Wavelengths (Å)	
Anode	$K\alpha_1$	$K\alpha_2$
Cu	1·54053$_6$	1·54435$_6$
Co	1·78895$_0$	1·79281$_0$
Fe	1·93600$_3$	1·93994$_3$

Values of $\sin \theta$ were obtained from Peters' (1942) tables and converted to $\sin \theta / \lambda$ values using the appropriate wavelength from Table 1.

2·4. *Computation of results*

The use of general reflections for obtaining reciprocal-lattice parameters has been discussed by Weisz, Cochran & Cole (1948); their method, in which the initially assumed values of the reciprocal-lattice parameters are refined by an iterative procedure, has been followed here. However the amount of numerical work required has been reduced by deriving initial values of the parameters from the high-angle reflections on the back-reflection Weissenberg photographs themselves. (Weisz *et al.* had used axial lengths from layer-line photographs as their starting values.) The method is illustrated for the $h0l$ zone of a triclinic or monoclinic crystal.

Let
$$Q_{h0l} = (2 \sin \theta / \lambda)^2_{h0l} .$$
Then
$$Q_{h0l} + Q_{h0\bar{l}} = 2(h^2(a^*)^2 + l^2(c^*)^2) \qquad (1)$$

$$Q_{h0l} - Q_{h0\bar{l}} = 4hla^*c^* \cos \beta^*. \qquad (2)$$

Equation (1) is linear in $(a^*)^2$ and $(c^*)^2$ and the set of equations obtained from the available $h0l$, $h0\bar{l}$ pairs can be solved graphically or, more accurately, by least squares. $\cos \beta^*$ is then obtained from equation (2), using these approximate values of a^* and c^*.

The iterative calculations are obviously well suited

to an electronic computer and appropriate programmes for triclinic and monoclinic crystals (this covers all symmetries required) have been written for the Stantec Zebra computer in this Laboratory.

3. Rotation photographs using the Mathieson film mounting

3·1. *Introduction*

Once a crystal has been set up about a particular axis for a series of Weissenberg photographs, it is convenient to be able to determine the value of the identity period along the rotation axis without remounting. This can be done with layer-line photographs to an accuracy of about 1%, but Mathieson (1957) has demonstrated that a marked increase in accuracy (to 0·1% was claimed) could be obtained if the film was mounted so that all the layer-lines could be recorded. In this arrangement the axis of the cylindrical strip of film is that normal to the crystal-rotation axis which lies in the plane defined by the X-ray beam and crystal rotation axis. The axis of the film must pass through the centre of the crystal. This definition applies to both normal- and inclined-beam rotation photographs. Thus for normal-beam photographs the X-ray beam is the axis of the cylindrical film strip. Mathieson's film-holder was designed to fit the Unicam S.25 goniometer and was thus limited to normal-beam rotation photographs; however the potential advantages of inclined-beam photographs were mentioned.

A film-holder using the Mathieson mounting has been designed to fit the Weissenberg film-holder and can therefore be used for inclined- as well as normal-beam rotation photographs. The processing of the measurements and the theory of the extrapolation required for the elimination of the eccentricity error are discussed below for inclined-beam photographs.

3·2. *Design and adjustment of film-holder*

The film-holder is shown in Fig. 4. Its dimensions
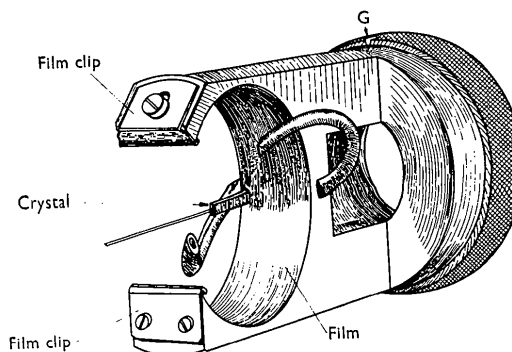
Fig. 4. Film holder for Mathieson film mounting. Internal diameter of film cylinder 2″. Heating/cooling device inserted from right, blowing gas through copper tubes onto the crystal. A pin on the Weissenberg film holder fits into groove G and holds the adaptor in the correct angular position.

are such that its centre will coincide with that of the Weissenberg film-holder, while it is held in the correct angular position by a stop. The adjustment of the film-holder centre to the position of the crystal is made as follows. Both Mathieson film-holder and crystal are removed from the camera. A pin is now passed through a small hole drilled through the top of the Weissenberg film-holder above its centre and is viewed through the collimator with a suitable lens. The carriage (to which the Weissenberg film-holder is clamped) is then shifted until the point of the pin is at the centre of the collimator and thus also at the crystal position. The carriage can be clamped in this position. Any residual error is minimized by the extrapolation procedure described below. It has been found necessary to attach the crystals to glass fibres about 17 mm. long in order that the arcs should not hit the Mathieson film-holder*.

The temperature regulators mentioned previously (Section 2·1) fit into the outer end of the Mathieson film-holder and gas of required temperature can be blown over the crystal. The design of the beam stop is also mentioned briefly in Section 2·1.

3·3. Theory of method

The formation of the diffraction cones for the normal- and inclined-beam situations ($\mu \neq 0$) is shown in Figs. 5(a) and (b). The standard equation (Buerger, 1942, p. 31) relating the semi-angles of the diffraction cones to the angle of incidence is

$$\cos \bar{\nu}_m = \cos \bar{\mu} + m\lambda/a$$

where a is the identity period along the crystal rotation axis and $\bar{\nu}_m$ is the semi-angle of the mth diffraction cone.

Now $\nu_m = \frac{1}{2}\pi - \bar{\nu}_m$; $\mu = \bar{\mu} - \frac{1}{2}\pi$. It follows at once that

$$a = m\lambda/(\sin \nu_m + \sin \mu) . \qquad (3)$$

When $\mu = 0$ this reduces to the usual equation for normal-beam photographs; $a = m\lambda/\sin \nu_m$.

The relations between distances on the film and $\bar{\nu}_m$ angles can be derived from Figs. 6(a) and (b). The inclined-beam situation is shown in Fig. 6(b), from which it follows that

$$l_m/l_o = \bar{\nu}_m/(\mu + \tfrac{1}{2}\pi) \qquad (4)$$

where l_m, l_o are the measured distances corresponding to the mth and zero layer-lines respectively. Thus

$$\nu_m = 90 - (90 + \mu)l_m/l_o \text{ degrees} . \qquad (5)$$

For $\mu = 0$ (Fig. 6(a)) this reduces to $\nu_m = 90[1 - (l_m/l_o)]$ degrees. It is clear from (5) that, with this film mounting, knowledge of the film radius is not required for the derivation of diffraction-cone semi-angles

---

* This applies to Nonius arcs.
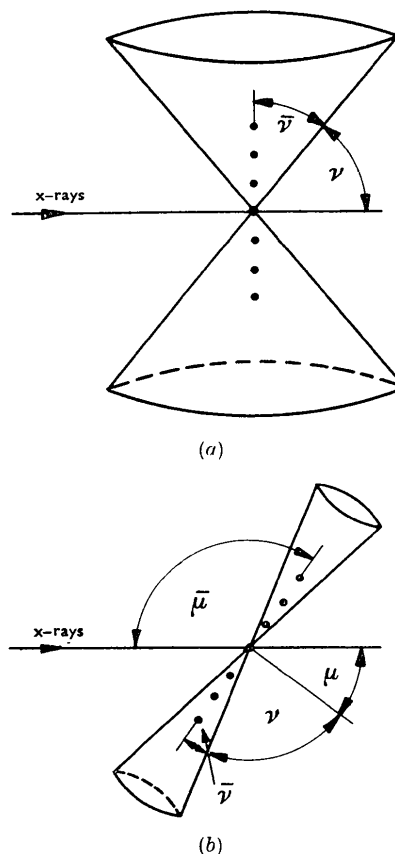
Fig. 5. Formation of diffraction cones for (a) normal-beam and (b) inclined-beam rotation photographs. In (a) the second-order diffraction cone ($\nu = 50°$) is shown and in (b) the fourth-order diffraction cone ($\nu = 78°$ for $\mu = 34°$). The repetition period along the crystal rotation axis is 4 Å and the wavelength 1·54 Å. The cylindrical film strip is mounted axially about that normal to the crystal rotation axis which lies in the same plane as the X-ray beam and the crystal rotation axis.

from measured distances; in this respect it resembles the Straumanis method.

3·4. Correction for eccentricity errors

The most important source of systematic error (Mathieson, 1957) is lack of coincidence of film centre and crystal along the direction of the crystal rotation axis (Fig. 7). The form of the extrapolation function can be derived by a method similar to that used by Mathieson for normal-beam photographs.

From Fig. 6(b)

$$l_o = 2r_0(\tfrac{1}{2}\pi + \mu)$$
$$l_m = 2\bar{\nu}_m r_0$$

while from Fig. 7

$$l'_o = 2[r_0(\tfrac{1}{2}\pi + \mu) - p \cos \mu]$$
$$l'_m = 2[r_0(\tfrac{1}{2}\pi - \nu_m) - p \cos \nu_m] .$$

(The dashed values indicate that the crystal is displaced off the film centre.)
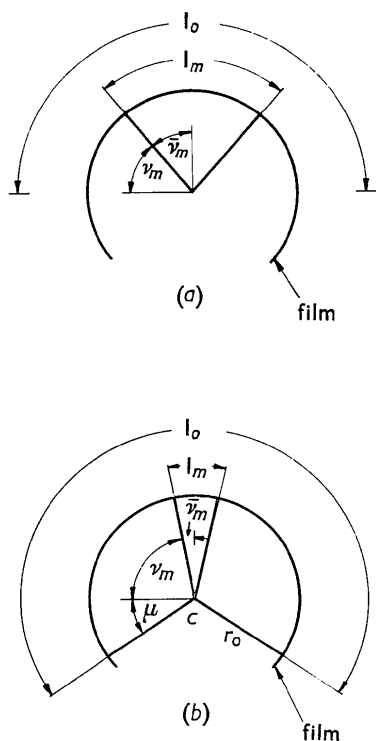
Fig. 6. Relation between distances l_o, l_m measured along the film and diffraction-cone semi-angles for (a) normal-beam and (b) inclined-beam rotation photographs. The same diffraction cones are shown as in Fig. 5.

Now let $\Delta \nu = \nu - \nu'$. Using the values above, and dropping the subscripts, one obtains

$$\Delta \nu = p \frac{(\frac{1}{2}\pi - \nu) \cos \mu - (\frac{1}{2}\pi + \mu) \cos \nu}{r_o (\frac{1}{2}\pi + \mu) - p \cos \mu} .$$

From (3)

$$\Delta a/a = - \frac{\cos \nu \Delta \nu}{(\sin \nu + \sin \mu)} \tag{6}$$

$$= \frac{p}{r_o(\frac{1}{2}\pi + \mu) - p \cos \mu}$$

$$\times \left\{ \frac{\cos \nu [(\frac{1}{2}\pi + \mu) \cos \nu - (\frac{1}{2}\pi - \nu) \cos \mu]}{\sin \nu + \sin \mu} \right\}$$

$$= \frac{p}{r_o(\frac{1}{2}\pi + \mu) - p \cos \mu} g(\mu, \nu) . \tag{7}$$

When $\mu = 0$ equation (7) becomes

$$\Delta a/a = \frac{\pi p}{\pi r_o - 2p} \left(1 - \frac{2}{\pi} \frac{\frac{1}{2}\pi - \nu}{\cos} \right) \cos^2 \nu \operatorname{cosec} \nu$$

which is Mathieson's extrapolation function $f(\nu)$.

$g(\mu, \nu)$ has been calculated for $\mu = 0°$ (1°) 40° and $= -55°$ (5°) 90° on the Stantec Zebra computer and the results are given in Table 2.

The validity of the extrapolation function has been tested by making six different measurements of the b spacing of hexabromobenzene. The results, plotted against $g(\mu, \nu)$, are shown in Fig. 8. Although the
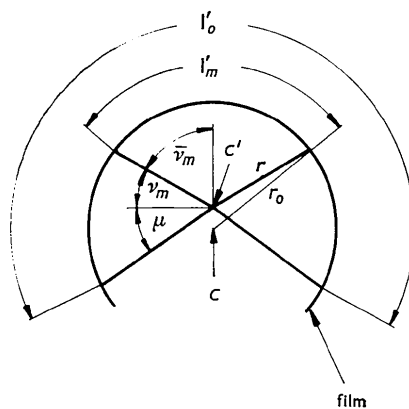
Fig. 7. The eccentricity error and its effects. The centre of the cylindrical film is at C while the crystal is at C'; $CC' = p$ and $r \sim r_0 - p \cos \bar{\nu}_m$ for small p.
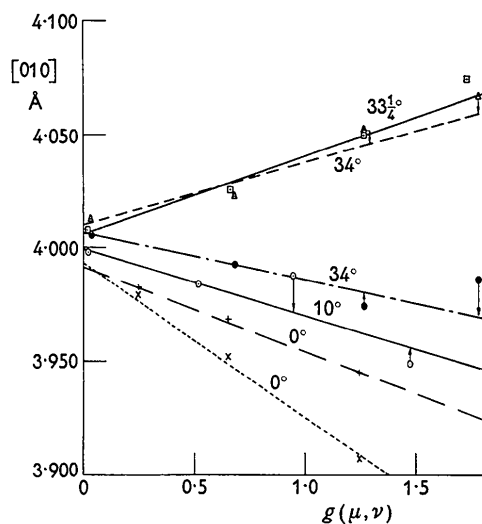
Fig. 8. Experimental values of [010] for hexabromobenzene plotted against $g(\mu, \nu)$. The measured values were derived from a number of different normal- and inclined-beam photographs (the film-holder was readjusted between photographs but the crystal settings were left unchanged). The inclination angles (μ) are shown in the diagram.

graphs have rather different slopes (corresponding to extreme values of p of about $\frac{1}{2}$ mm), the intercepts all lie in the limits 3·991–4·010 Å, with the mean value 4·002 ± 0·003 Å. Failure to use the $g(\mu, \nu)$ extrapolation function may give misleading results.

3·5. Weighting of results

The values of the identity period deduced from the different layer-lines are plotted against $g(\mu, \nu)$ and the extrapolated value at $\nu = 90°$ obtained by least squares. The weights assigned to these values were calculated assuming random errors in the measurement of l_m. Repeated measurements on individual films suggest that $dl_m \sim 0·3$ mm for $\nu < 70°$, but about 1 mm for $\nu > 70°$. The worsening of the spot shape is due partly to the finite size of the crystals

Table 2. Values of $g(\mu, \nu)$

$\nu \rightarrow$

$\mu \downarrow$	-55	-50	-45	-40	-35	-30	-25	-20	-15	-10	-5	0	5	10	15
0	1.1412	1.2031	1.2455	1.2700	1.2781	1.2714	1.2513	1.2193	1.1768	1.1252	1.0658	1.0000	0.9291	0.8545	0.7773
1	1.1586	1.2212	1.2640	1.2886	1.2967	1.2897	1.2692	1.2366	1.1933	1.1408	1.0805	1.0138	0.9419	0.8661	0.7878
2	1.1762	1.2395	1.2827	1.3074	1.3154	1.3081	1.2872	1.2539	1.2100	1.1566	1.0954	1.0276	0.9547	0.8778	0.7984
3	1.1940	1.2580	1.3016	1.3265	1.3343	1.3268	1.3053	1.2715	1.2267	1.1726	1.1104	1.0416	0.9676	0.8896	0.8091
4	1.2120	1.2767	1.3207	1.3457	1.3534	1.3456	1.3236	1.2892	1.2437	1.1886	1.1255	1.0557	0.9806	0.9015	0.8199
5	1.2303	1.2956	1.3400	1.3651	1.3728	1.3646	1.3421	1.3070	1.2607	1.2048	1.1408	1.0699	0.9937	0.9135	0.8307
6	1.2487	1.3148	1.3595	1.3847	1.3923	1.3837	1.3608	1.3250	1.2780	1.2211	1.1561	1.0842	1.0069	0.9256	0.8416
7	1.2675	1.3341	1.3792	1.4046	1.4120	1.4031	1.3796	1.3432	1.2953	1.2376	1.1715	1.0986	1.0202	0.9377	0.8526
8	1.2864	1.3538	1.3992	1.4246	1.4319	1.4227	1.3987	1.3615	1.3129	1.2542	1.1871	1.1131	1.0336	0.9500	0.8637
9	1.3056	1.3736	1.4194	1.4449	1.4520	1.4424	1.4179	1.3800	1.3306	1.2710	1.2029	1.1277	1.0471	0.9623	0.8749
10	1.3250	1.3937	1.4399	1.4654	1.4723	1.4624	1.4373	1.3987	1.3484	1.2880	1.2187	1.1425	1.0607	0.9748	0.8861
11	1.3447	1.4141	1.4606	1.4862	1.4929	1.4825	1.4569	1.4176	1.3664	1.3049	1.2348	1.1574	1.0745	0.9873	0.8975
12	1.3647	1.4347	1.4815	1.5072	1.5137	1.5029	1.4767	1.4367	1.3846	1.3222	1.2509	1.1724	1.0883	1.0000	0.9089
13	1.3850	1.4556	1.5027	1.5284	1.5347	1.5235	1.4967	1.4559	1.4030	1.3395	1.2672	1.1876	1.1023	1.0127	0.9204
14	1.4055	1.4768	1.5242	1.5499	1.5560	1.5444	1.5169	1.4754	1.4215	1.3571	1.2836	1.2029	1.1164	1.0256	0.9320
15	1.4263	1.4982	1.5459	1.5716	1.5775	1.5654	1.5373	1.4950	1.4402	1.3748	1.3002	1.2183	1.1306	1.0386	0.9438
16	1.4474	1.5199	1.5679	1.5937	1.5993	1.5867	1.5580	1.5148	1.4591	1.3926	1.3170	1.2339	1.1449	1.0516	0.9556
17	1.4688	1.5420	1.5902	1.6160	1.6213	1.6083	1.5788	1.5349	1.4782	1.4107	1.3339	1.2496	1.1594	1.0648	0.9675
18	1.4906	1.5643	1.6129	1.6385	1.6436	1.6300	1.5999	1.5551	1.4975	1.4289	1.3510	1.2654	1.1739	1.0781	0.9795
19	1.5126	1.5870	1.6358	1.6614	1.6661	1.6521	1.6213	1.5756	1.5170	1.4473	1.3682	1.2814	1.1887	1.0915	0.9916
20	1.5350	1.6100	1.6590	1.6846	1.6890	1.6744	1.6428	1.5963	1.5367	1.4659	1.3856	1.2976	1.2035	1.1051	1.0038
21	1.5578	1.6333	1.6825	1.7080	1.7121	1.6969	1.6647	1.6173	1.5566	1.4847	1.4032	1.3139	1.2185	1.1187	1.0161
22	1.5809	1.6570	1.7064	1.7318	1.7355	1.7198	1.6867	1.6384	1.5768	1.5036	1.4209	1.3303	1.2336	1.1325	1.0285
23	1.6043	1.6810	1.7306	1.7559	1.7592	1.7429	1.7091	1.6598	1.5971	1.5228	1.4388	1.3470	1.2489	1.1464	1.0411
24	1.6282	1.7054	1.7552	1.7803	1.7832	1.7663	1.7317	1.6815	1.6176	1.5422	1.4569	1.3637	1.2643	1.1605	1.0537
25	1.6524	1.7301	1.7801	1.8051	1.8076	1.7900	1.7545	1.7034	1.6384	1.5618	1.4752	1.3807	1.2799	1.1746	1.0665
26	1.6771	1.7553	1.8054	1.8302	1.8323	1.8140	1.7777	1.7255	1.6595	1.5816	1.4937	1.3978	1.2956	1.1889	1.0794
27	1.7021	1.7808	1.8311	1.8557	1.8573	1.8383	1.8012	1.7479	1.6807	1.6016	1.5124	1.4151	1.3115	1.2034	1.0924
28	1.7276	1.8068	1.8571	1.8815	1.8826	1.8630	1.8249	1.7706	1.7022	1.6218	1.5313	1.4326	1.3275	1.2180	1.1055
29	1.7535	1.8332	1.8836	1.9077	1.9083	1.8879	1.8489	1.7936	1.7240	1.6423	1.5504	1.4502	1.3437	1.2327	1.1188
30	1.7799	1.8600	1.9105	1.9343	1.9344	1.9132	1.8733	1.8168	1.7460	1.6629	1.5697	1.4681	1.3601	1.2476	1.1322
31	1.8067	1.8873	1.9378	1.9613	1.9608	1.9389	1.8979	1.8403	1.7683	1.6839	1.5892	1.4861	1.3767	1.2626	1.1457
32	1.8341	1.9150	1.9655	1.9887	1.9876	1.9649	1.9229	1.8642	1.7908	1.7050	1.6089	1.5044	1.3934	1.2778	1.1593
33	1.8619	1.9433	1.9937	2.0166	2.0148	1.9912	1.9482	1.8883	1.8136	1.7265	1.6288	1.5228	1.4103	1.2931	1.1731
34	1.8903	1.9720	2.0224	2.0449	2.0425	2.0180	1.9739	1.9127	1.8367	1.7481	1.6490	1.5414	1.4273	1.3086	1.1870
35	1.9192	2.0012	2.0515	2.0736	2.0706	2.0451	1.9999	1.9375	1.8601	1.7701	1.6694	1.5603	1.4446	1.3242	1.2011
36	1.9487	2.0310	2.0812	2.1028	2.0990	2.0726	2.0263	1.9626	1.8838	1.7923	1.6901	1.5793	1.4620	1.3401	1.2153
37	1.9787	2.0613	2.1113	2.1325	2.1279	2.1005	2.0530	1.9880	1.9078	1.8148	1.7110	1.5986	1.4797	1.3560	1.2297
38	2.0093	2.0922	2.1420	2.1626	2.1572	2.1288	2.0802	2.0138	1.9321	1.8375	1.7322	1.6181	1.4975	1.3722	1.2442
39	2.0406	2.1236	2.1733	2.1933	2.1871	2.1576	2.1077	2.0399	1.9568	1.8606	1.7536	1.6379	1.5155	1.3886	1.2589
40	2.0725	2.1557	2.2051	2.2244	2.2174	2.1868	2.1356	2.0664	1.9817	1.8839	1.7752	1.6578	1.5338	1.4051	1.2737

$\nu \rightarrow$

$\mu \downarrow$	20	25	30	35	40	45	50	55	60	65	70	75	80	85	90
0	0.6988	0.6201	0.5424	0.4667	0.3940	0.3253	0.2614	0.2031	0.1511	0.1061	0.0685	0.0388	0.0173	0.0043	0.0
1	0.7082	0.6284	0.5497	0.4729	0.3993	0.3296	0.2649	0.2058	0.1531	0.1075	0.0694	0.0393	0.0175	0.0044	0.0
2	0.7177	0.6368	0.5570	0.4792	0.4046	0.3340	0.2684	0.2085	0.1552	0.1089	0.0703	0.0398	0.0178	0.0045	0.0
3	0.7273	0.6453	0.5643	0.4855	0.4099	0.3384	0.2719	0.2113	0.1572	0.1103	0.0712	0.0403	0.0180	0.0045	0.0
4	0.7369	0.6538	0.5718	0.4919	0.4152	0.3428	0.2754	0.2140	0.1592	0.1117	0.0721	0.0408	0.0182	0.0046	0.0
5	0.7466	0.6624	0.5792	0.4983	0.4206	0.3472	0.2790	0.2167	0.1613	0.1132	0.0731	0.0414	0.0185	0.0046	0.0
6	0.7564	0.6710	0.5867	0.5047	0.4261	0.3517	0.2826	0.2195	0.1633	0.1146	0.0740	0.0419	0.0187	0.0047	0.0
7	0.7662	0.6797	0.5943	0.5112	0.4315	0.3562	0.2862	0.2223	0.1654	0.1161	0.0749	0.0424	0.0189	0.0048	0.0
8	0.7761	0.6884	0.6019	0.5178	0.4370	0.3607	0.2898	0.2251	0.1675	0.1175	0.0759	0.0430	0.0192	0.0048	0.0
9	0.7861	0.6973	0.6096	0.5243	0.4425	0.3653	0.2934	0.2280	0.1696	0.1190	0.0768	0.0435	0.0194	0.0049	0.0
10	0.7962	0.7061	0.6173	0.5310	0.4481	0.3698	0.2971	0.2308	0.1717	0.1205	0.0778	0.0440	0.0197	0.0049	0.0
11	0.8063	0.7151	0.6251	0.5376	0.4537	0.3745	0.3008	0.2337	0.1738	0.1220	0.0787	0.0446	0.0199	0.0050	0.0
12	0.8165	0.7241	0.6330	0.5444	0.4594	0.3791	0.3045	0.2366	0.1760	0.1235	0.0797	0.0451	0.0202	0.0051	0.0
13	0.8268	0.7332	0.6409	0.5511	0.4651	0.3838	0.3083	0.2395	0.1781	0.1250	0.0807	0.0457	0.0204	0.0051	0.0
14	0.8372	0.7423	0.6488	0.5579	0.4708	0.3885	0.3121	0.2424	0.1803	0.1265	0.0817	0.0462	0.0206	0.0052	0.0
15	0.8476	0.7516	0.6569	0.5648	0.4766	0.3933	0.3159	0.2453	0.1825	0.1280	0.0826	0.0468	0.0209	0.0052	0.0
16	0.8582	0.7609	0.6650	0.5717	0.4824	0.3980	0.3197	0.2483	0.1847	0.1296	0.0836	0.0474	0.0211	0.0053	0.0
17	0.8688	0.7702	0.6731	0.5787	0.4883	0.4029	0.3236	0.2513	0.1869	0.1311	0.0846	0.0479	0.0214	0.0054	0.0
18	0.8795	0.7797	0.6813	0.5858	0.4942	0.4077	0.3275	0.2543	0.1891	0.1327	0.0857	0.0485	0.0217	0.0054	0.0
19	0.8903	0.7892	0.6896	0.5928	0.5001	0.4126	0.3314	0.2573	0.1914	0.1343	0.0867	0.0491	0.0219	0.0055	0.0
20	0.9012	0.7988	0.6980	0.6000	0.5061	0.4176	0.3353	0.2604	0.1937	0.1359	0.0877	0.0496	0.0222	0.0056	0.0
21	0.9122	0.8085	0.7064	0.6072	0.5122	0.4225	0.3393	0.2635	0.1959	0.1375	0.0887	0.0502	0.0224	0.0056	0.0
22	0.9233	0.8182	0.7149	0.6144	0.5183	0.4275	0.3433	0.2666	0.1983	0.1391	0.0898	0.0508	0.0227	0.0057	0.0
23	0.9345	0.8281	0.7234	0.6218	0.5244	0.4326	0.3473	0.2697	0.2006	0.1407	0.0908	0.0514	0.0230	0.0058	0.0
24	0.9457	0.8380	0.7320	0.6291	0.5306	0.4377	0.3514	0.2729	0.2029	0.1423	0.0919	0.0520	0.0232	0.0058	0.0
25	0.9571	0.8480	0.7407	0.6366	0.5369	0.4428	0.3555	0.2760	0.2053	0.1440	0.0929	0.0526	0.0235	0.0059	0.0
26	0.9686	0.8582	0.7495	0.6441	0.5431	0.4480	0.3597	0.2792	0.2076	0.1457	0.0940	0.0532	0.0238	0.0060	0.0
27	0.9802	0.8684	0.7584	0.6516	0.5495	0.4532	0.3638	0.2825	0.2100	0.1473	0.0951	0.0538	0.0240	0.0060	0.0
28	0.9919	0.8786	0.7673	0.6593	0.5559	0.4584	0.3680	0.2857	0.2124	0.1490	0.0962	0.0544	0.0243	0.0061	0.0
29	1.0037	0.8890	0.7763	0.6670	0.5624	0.4637	0.3723	0.2890	0.2149	0.1507	0.0973	0.0551	0.0246	0.0062	0.0
30	1.0156	0.8995	0.7854	0.6747	0.5689	0.4691	0.3765	0.2923	0.2173	0.1524	0.0984	0.0557	0.0249	0.0062	0.0
31	1.0276	0.9101	0.7946	0.6826	0.5754	0.4745	0.3809	0.2956	0.2198	0.1542	0.0995	0.0563	0.0251	0.0063	0.0
32	1.0398	0.9208	0.8038	0.6905	0.5821	0.4799	0.3852	0.2990	0.2223	0.1559	0.1006	0.0569	0.0254	0.0064	0.0
33	1.0520	0.9315	0.8132	0.6985	0.5888	0.4854	0.3896	0.3024	0.2248	0.1577	0.1017	0.0576	0.0257	0.0064	0.0
34	1.0644	0.9424	0.8226	0.7065	0.5955	0.4909	0.3940	0.3058	0.2273	0.1594	0.1029	0.0582	0.0260	0.0065	0.0
35	1.0769	0.9534	0.8321	0.7146	0.6023	0.4965	0.3985	0.3093	0.2299	0.1612	0.1040	0.0589	0.0263	0.0066	0.0
36	1.0896	0.9645	0.8417	0.7228	0.6092	0.5022	0.4030	0.3128	0.2325	0.1630	0.1052	0.0595	0.0266	0.0067	0.0
37	1.1023	0.9757	0.8515	0.7311	0.6161	0.5079	0.4075	0.3163	0.2351	0.1649	0.1064	0.0602	0.0269	0.0067	0.0
38	1.1152	0.9870	0.8613	0.7395	0.6231	0.5136	0.4121	0.3198	0.2377	0.1667	0.1075	0.0609	0.0272	0.0068	0.0
39	1.1282	0.9984	0.8712	0.7479	0.6302	0.5194	0.4167	0.3234	0.2404	0.1685	0.1087	0.0615	0.0275	0.0069	0.0
40	1.1414	1.0100	0.8812	0.7564	0.6373	0.5253	0.4214	0.3270	0.2430	0.1704	0.1099	0.0622	0.0278	0.0070	0.0

used but $\alpha_1-\alpha_2$ splitting is also an important contributing factor. From (6) it follows that weights are proportional to $[(\sin \nu + \sin \mu)/\cos \nu d\nu]^2$, which reduces to $(\tan \nu/d\nu)^2$ for normal-beam photographs. ($d\nu_m$ is obtained from dl_m by differentiation of (5)).

4. Treatment of errors

The errors in the dimensions of the crystal lattice can be derived in terms of the errors in the measured reciprocal-lattice parameters. The errors in interatomic distances can then be derived in terms of the errors in the dimensions of the crystal lattice.

Both these derivations depend on the following well-known theorem in the theory of errors:

if $y = F(x_1, x_2, \ldots, x_n)$

then $\sigma^2(y) = \sum_{i=1}^{n} (\partial F/\partial x_i)^2 \sigma^2(x_i)$ (8)

where $\sigma^2(y)$ and $\sigma^2(x_i)$ are the variances of the dependent and independent variables respectively. This treatment assumes that the covariances of the various errors are zero.

4·1. Errors in cell dimensions due to errors in measured parameters

In a triclinic crystal a and $\cos \alpha$ are given by

$$a = d_{100} \operatorname{cosec} \beta^* \operatorname{cosec} \gamma^*$$
$$\cos \alpha = (\cos \beta^* \cos \gamma^* - \cos \alpha^*)/\sin \beta^* \sin \gamma^*.$$

The equations for $b, c, \cos\beta, \cos\gamma$ are obtained by cyclic permutation. From equation (8) it follows that

$$\sigma(a)/a = [\sigma^2(d_{100})/d_{100}^2 + \cot^2\beta \, \sigma^2(\beta) + \cot^2\gamma^* \sigma^2(\gamma^*)]^{\frac{1}{2}} \quad (9)$$

$$\sigma(\cos \alpha) = \operatorname{cosec} \beta^* \operatorname{cosec} \gamma^* \left[\sin^2 \alpha^* \sigma^2(\alpha^*) \right.$$
$$+ \left(\frac{\cos \alpha^* \cos \beta^* - \cos \gamma^*}{\sin \beta^*} \right)^2 \sigma^2(\beta^*)$$
$$+ \left. \left(\frac{\cos \alpha^* \cos \gamma^* - \cos \beta^*}{\sin \gamma^*} \right)^2 \sigma^2(\gamma^*) \right]^{\frac{1}{2}}. \quad (10)$$

The corresponding equations for the other cell dimensions are obtained in the same way. Equations (9) and (10) become simpler for crystal systems of higher symmetry.

The angles are often obtained through $\cos \alpha$ etc. rather than directly. It is therefore useful to list as well

$$\sigma(\alpha) = \operatorname{cosec} \alpha \sigma (\cos \alpha) . \quad (11)$$

4.2. Errors in interatomic distances due to errors in cell dimensions

In a triclinic crystal the distance q_{rs} between two points r, s at x_{ri}, x_{si} ($i = 1, 2, 3$) is given by

$$q_{rs}^2 = \sum_{i=1}^{3} (x_{ri} - x_{si})^2 + 2 \sum_{i=1}^{3} \sum_{j=i+1}^{3} (x_{ri} - x_{si})$$
$$\times (x_{rj} - x_{sj}) \cos \varphi_{ij} \quad (12)$$

where φ_{ij} is the angle between axes $\mathbf{a}_i, \mathbf{a}_j$. We now define

$$x_{ri} - x_{si} \equiv a_i (u_{ri} - u_{si}) \equiv a_i \Delta u_i$$

where u_{ri}, u_{si} are the fractional co-ordinates of atoms r, s. The errors in the fractional co-ordinates due to errors in cell dimensions will be negligibly small. Equation (12) becomes

$$q_{rs}^2 = \sum_{i=1}^{3} a_i^2 (\Delta u_i)^2$$
$$+ 2 \sum_{i=1}^{3} \sum_{j=i+1}^{3} a_i a_j \Delta u_i \Delta u_j \cos \varphi_{ij} . \quad (13)$$

Using (8) it follows that

$$\sigma^2(q_{rs}) = q_{rs}^{-2} \left\{ \sum_{i=1}^{3} [\Delta u_i \sum_{j=1}^{3} a_j \Delta u_j \cos \varphi_{ij}]^2 \sigma^2(a_i) \right.$$
$$+ \sum_{i=1}^{3} \sum_{j=i+1}^{3} [a_i a_j \Delta u_i \Delta u_j \sin \varphi_{ij}]^2 \sigma^2(\varphi_{ij}) . \quad (14)$$

It should be noted that $\varphi_{ii} = 0$ in the first term. There are considerable simplifications for higher-symmetry crystal systems.

5. Results

Results given below for hexabromobenzene are typical of those obtained for a number of substances. Preliminary crystallographic data have been reported for this compound (Gafner & Herbstein, 1960) but more
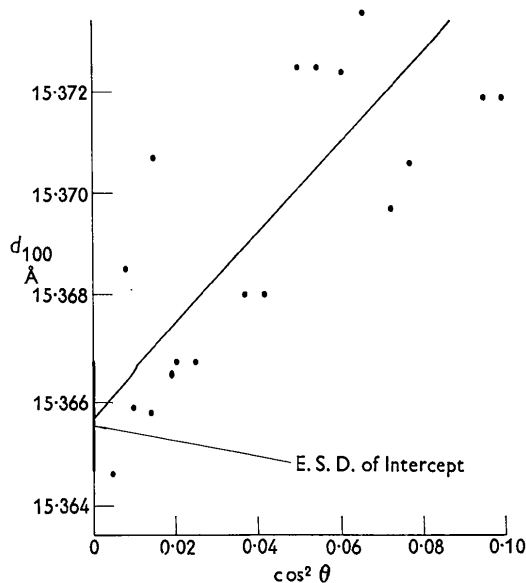

Fig. 9. Graph of d_{100} against $\cos^2 \theta$ for hexabromobenzene at 20 °C. (measurements from back-reflexion Weissenberg photograph about [010]). Weights assigned on the basis of random errors only i.e. $W_{hol} \propto \tan^2 \theta_{hol}$.

accurate values were required for a study of oriented overgrowth (Boonstra & Herbstein, 1963). The sample used was obtained from Dr Th. J. de Boer (University of Amsterdam) and was recrystallized once from toluene.

Accurate values of the cell dimensions were determined at 20 °C. as follows. A back-reflection Weissenberg photograph was taken (Cu $K\alpha$) of a crystal rotating about the needle axis [010]. Analysis of this photograph gave directly $d_{100} = 15\cdot3657 \pm 0\cdot0010$ Å, $d_{001} = 8\cdot3676 \pm 0\cdot0006$ Å and $\cos\beta^* = 0\cdot04694 \pm 0\cdot00006$. A typical extrapolation graph is shown in Fig. 9. The cell dimensions derived from these parameters were as follows:

$$a = 15\cdot3816 \pm 0\cdot0010, \quad c = 8\cdot3768 \pm 0\cdot0006 \text{ Å};$$
$$\beta = 92\cdot691 \pm 0\cdot004°.$$

The b value was determined from two normal- and four inclined-beam rotation photographs using the Mathieson film mounting (Fig. 8). The final value was taken as the mean of these individual values and was $4\cdot002 \pm 0\cdot003$ Å. The relative accuracy of b is more than an order of magnitude worse than for the other results. It is worth noting that the method used for determining d_{100}, d_{001} and $\cos\beta^*$ from the $h0l$ reflections is equally applicable to triclinic crystals.

Refraction corrections were not applied as these (Straumanis, 1955) would be much smaller than the errors of measurement.

6. Discussion

Under favourable conditions the back-reflection Weissenberg method gives measured cell dimensions with standard deviations of about 0·0025–0·01%. These standard deviations are about as large as those reported by Weisz et al. (1948) for the oscillating-crystal method (which is equivalent in principle to that used here) but are about an order of magnitude smaller than those obtained by Weisz et al. by the θ-method. Löfgren (1961) has pointed out that use of extrapolation procedures leads to a considerable improvement in the accuracy obtainable with the θ-method, although the standard deviation of his result ($d = 12\cdot945 \pm 0\cdot004$ Å) was about the same as the values given by Weisz et al. The capabilities of the θ-method are better illustrated by the results recently reported for orthorhombic sulphur by Cooper et al. (1961) using Bond's apparatus. The standard deviations were about 0·001%.

The back-reflection Weissenberg method described in this paper has advantages of convenience and accessibility and is found in practice to be not much less accurate than the best current applications of the θ-method. The major factor limiting its accuracy at present is the difficulty of measuring reflection angles to better than 0·02° in θ. Much greater sensitivity ($\sim 0\cdot002°$ in θ) could be obtained by using counters (Smakula & Kalnajs, 1955) but the resulting complications would largely negate the present advantages of the method. If greater accuracy is required then the θ-method as used by Bond is undoubtedly to be preferred. On the other hand, judging from the published data, the film version of the θ-method does not appear to give results as accurate as those obtainable by the back-reflection Weissenberg method. The difference is probably due to the larger number of high-angle reflections which can be measured with the back-reflection Weissenberg method.

Mathieson-adaptor rotation photographs are convenient for determining identity periods, particularly if the inclined-beam method is used, but the accuracy attainable is limited (about 0·1%).

References

ABRAHAMS, S. C. (1961). Acta Cryst. **14**, 311.
BOND, W. L. (1960). Acta Cryst. **13**, 814.
BOONSTRA, E. G. & HERBSTEIN, F. H. (1963). Acta Cryst. **16**, 252.
BRAEKKEN, H. (1929). Det Kong. Nordiske Videnskabers Selskab. Forhand. **1**, No. 64.
BUERGER, M. J. (1937). Z. Kristallogr. A, **97**, 433.
BUERGER, M. J. (1942). X-ray Crystallography. New York: Wiley.
BUERGER, M. J. & PARRISH, W. (1937). Amer. Min. **22**, 1146.
CARON, A. & DONOHUE, J. (1961). Acta Cryst. **14**, 548.
CHRIST, C. L. (1956). Amer. Min. **41**, 569.
COOPER, A. S., BOND, W. L. & ABRAHAMS, S. C. (1961). Acta Cryst. **14**, 1008.
CRUICKSHANK, D. W. J. (1960). Acta Cryst. **13**, 774.
FARQUHAR, M. C. M. & LIPSON, H. (1946). Proc. Phys. Soc. **58**, 700.
FISCHMEISTER, H. (1951). Acta Phys. Austr. **5**, 254.
GAFNER, G. & HERBSTEIN, F. H. (1960). Acta Cryst. **13**, 702.
HERBSTEIN, F. H. (1957). Nature, Lond. **180**, 291.
KREUGER, A. (1955). Acta Cryst. **8**, 348.
LÖFGREN, T. (1961). Acta Cryst. **14**, 85.
LONSDALE, K. (1950). Acta Cryst. **3**, 400.
LONSDALE, K. (1959). Z. Kristallogr. **112**, 188.
MATHIESON, A. McL. (1957). Acta Cryst. **10**, 351.
PARRISH, W. (1960). Acta Cryst. **13**, 838.
PETERS, J. (1942). Seven-place Values of Trigonometric Functions. New York: Van Nostrand.
SMAKULA, A. & KALNAJS, J. (1955). Phys. Rev. **99**, 1737.
STRAUMANIS, M. E. (1955). Acta Cryst. **8**, 654.
WEISZ, O., COCHRAN, W. & COLE, W. F. (1948). Acta Cryst. **1**, 83.